2024 IEEE 63rd Conference on Decision and Control (CDC)
December 16-19, 2024. MiCo, Milan, Italy

Epigenetic cell memory: binary or analog?*

Simone Bruno[1,2] and Domitilla Del Vecchio[2]

Abstract— **Epigenetic cell memory is the property enabling multicellular organisms to keep distinct cell types despite sharing the same genotype. DNA methylation and histone modifications play a crucial role in maintaining the long-term memory of gene expression patterns specific to each cell type. Experimental results in semi-synthetic genetic systems show that these modifications silence and reactivate genes in an "all or none" manner, suggesting binary epigenetic memory (only extremal gene expression levels have long-term memory). However, in recent years, continuous and graded variations of gene expression levels have been identified across multiple cell types. Here, by introducing and analyzing a chromatin modification circuit model, we demonstrate that the experimentally observed bimodal probability distributions of gene expression level, used to support the binary memory hypothesis, are also compatible with the analog memory hypothesis, where cells can maintain any initially set gene expression level. Our study shows that intrinsic noise combined with an ultrasensitive response between the level of DNA methylation writer DNMT3A and DNA methylation grade at a gene can explain how analog epigenetic cell memory leads to a bimodal gene expression level distribution. The model can help design experiments to help distinguish between binary and analog memory, thereby offering a tool for interrogating the very essence of epigenetic cell memory.**

I. Introduction

Epigenetic cell memory (ECM) is the property of multicellular organisms to maintain different phenotypes despite sharing a common genetic sequence. This property is primarily influenced by the compaction of DNA structure (known as the chromatin state) [1], [2], regulated by epigenetic modifications to DNA and histones [1], [3]. More precisely, DNA methylation has been considered the essence of long-term memory, as it can persist through subsequent cell divisions by the action of enzymes that replicate the methylation pattern from the parental DNA strand onto the newly synthesized DNA strand during DNA replication [4].

In the past, experimental results suggested a genome-wide distribution of DNA methylation primarily concentrated at the extremal levels [5]–[7]. More recently, studies such as [8] support this notion, showing that chromatin modifiers transiently recruited to a gene influence the fraction of cells that are silenced or active, rather than directly affecting the gene expression level. Overall, these experimental results support the hypothesis of binary epigenetic cell memory (cells can stably maintain only silenced or active gene expression levels). However, in the past years, graded variations in gene expression levels have been observed across various cell types, such as the ones forming the mouse isocortex and hippocampus [9]. This suggests that cells must have a mechanism enabling them to maintain their specific gene expression level and associated identity.

Here, we explore how long-term memory of intermediate gene expression levels can be achieved and how chromatin modifications affect this process. Our goal is to demonstrate that the experimentally observed probability distributions of gene expression level, used to support the binary memory hypothesis, are also compatible with the analog memory hypothesis (cells can maintain any initially set gene expression level). To this end, we first introduce a mathematical model combining histone modifications and DNA methylation, and exploit Gillespie's Stochastic Simulation Algorithm [10] to understand how system's parameters qualitatively affect gene expression memory. Then, we derive a reduced order model recapitulating the mechanisms behind analog memory and use it to determine how experimental results are compatible with analog memory.

II. Chromatin modification circuit model

In this section, we briefly describe the chromatin modification circuit considered in our study, developed starting from the one in [11]. The chromatin modifications considered are H3K9 methylation (H3K9me3), H3K4 methylation (H3K4me3), and DNA methylation (DNAme). In terms of species, the model includes unmodified nucleosome (D), nucleosome with H3K4me3 ($\mathrm{D^A}$), with DNAme, ($\mathrm{D_1^R}$), with H3K9me3 ($\mathrm{D_2^R}$), or with both H3K9me3 and DNAme ($\mathrm{D_{12}^R}$). The reaction model can be represented by the circuit diagram shown in Fig. 1(a), with the corresponding reactions listed in Table I. More precisely, writer enzymes can *de novo establish* chromatin marks and histone modifications can recruit these enzymes to establish the same modification on nearby modifiable nucleosomes (*auto-catalysis*) [1], [12] (green, red, and light orange arrows in Fig. 1(a)). Furthermore, DNA methylation and H3K9me3 enhance

*This work was supported by NSF MODULUS Collaborative Research grant MCB-2027949.

[1]Department of Data Science, Dana-Farber Cancer Institute, Boston, MA, 02115, USA.

[2]Department of Mechanical Engineering, Massachusetts Institute of Technology, Cambridge, MA, 02139, USA.

Emails: sbruno@ds.dfci.harvard.edu, ddv@mit.edu

each other by recruiting each other's writer enzymes (*cross-catalysis*) [13] (red and light orange arrows in Fig. 1(a)). Eventually, these modifications are removed through dilution during DNA replication or by the action of eraser enzymes (*basal erasure*). Finally, activating modification erasers can be recruited by repressive modifications, and *viceversa* (*recruited erasure*) [14]–[16] (gray and dark orange arrows in Fig. 1(a)).

Let us now introduce the corresponding ordinary differential equation (ODE) model in terms of $\bar{D}^A = n^A/\mathrm{D_{tot}}$, $\bar{D}_1^R = n_{D_1^R}/\mathrm{D_{tot}}$, $\bar{D}_2^R = n_{D_2^R}/\mathrm{D_{tot}}$, $\bar{D}_{12}^R = n_{D_{12}^R}/\mathrm{D_{tot}}$ and $\bar{D} = n_D/\mathrm{D_{tot}}$, with $\mathrm{D_{tot}}$ representing the total number of nucleosomes in the gene, and n^A, n_1^R, n_2^R, n_{12}^R, and n^D denoting the amount of $\mathrm{D^A}, \mathrm{D_1^R}, \mathrm{D_2^R}, \mathrm{D_{12}^R}, \mathrm{D}$. It is possible to do this by assuming $\mathrm{D_{tot}}$ large enough to consider $\bar{D}^A$, $\bar{D}_1^R$, $\bar{D}_2^R$, $\bar{D}_{12}^R$ and $\bar{D}$ real numbers. Now, let us introduce $D_{tot} = \mathrm{D_{tot}}/\Omega$, with Ω denoting the reaction volume, and the normalized inputs: $u_{i0}^R = k_{W0}^i/k_M^A D_{tot}$, $u_i^R = k_W^i/(k_M^A D_{tot})$, $u_0^A = k_{W0}^A/(k_M^A D_{tot})$, and $u^A = k_W^A/(k_M^A D_{tot})$, with $i = 1, 2$. Additionally, let

$$\alpha = k_M/k_M^A, \quad \alpha' = k'_M/k_M^A, \quad \bar{\alpha} = \bar{k}_M/k_M^A. \tag{1}$$

The parameter α ($\bar{\alpha}$, α') is the non-dimensional rate constant associated with auto-catalysis (cross-catalysis). We consider α' (α, $\bar{\alpha}$) to be the same whether the nucleosome to be modified with DNAme (H3K9me3) is unmodified or already modified with H3K9me3 (DNAme). This will not affect the qualitative results obtained in this work. Finally, let

$$\varepsilon = \frac{\delta + \bar{k}_E^A}{k_M^A D_{tot}}, \quad \varepsilon' = \frac{k_E^A}{k_M^A}, \quad \mu' = \frac{k_T^{'*}}{k_E^A}, \quad \mu = \frac{k_E^R}{k_E^A}, \tag{2}$$

with $\beta = O(1)$ such that $(\delta' + k'_T)/(\delta + \bar{k}_E^A) = \beta\mu'$, and, similarly, $b = O(1)$ such that $(\delta + \bar{k}_E^R)/(\delta + \bar{k}_E^A) = b\mu$. Then, μ' (μ) quantifies the relative speed between the rate of DNA demethylation (H3K9me3 erasure rate) and H3K4me3 erasure rate and ε (ε') is a parameter that scales the ratio between the rate of basal (recruited) erasure and the auto-catalysis rate of each modification. Finally, introducing the normalized time $\tau = t k_M^A D_{tot}$, the ODEs can be written as

$$\begin{aligned}
\frac{d\bar{D}_1^R}{d\tau} &= (u_{10}^R + u_1^R + \alpha'(\bar{D}_2^R + \bar{D}_{12}^R))\bar{D} + \mu(b\varepsilon + \varepsilon'\bar{D}^A)\bar{D}_{12}^R \\
&\quad - (u_{20}^R + \alpha(\bar{D}_2^R + \bar{D}_{12}^R) + \bar{\alpha}(\bar{D}_1^R + \bar{D}_{12}^R))\bar{D}_1^R \\
&\quad - \mu'(\beta\varepsilon + \varepsilon'\bar{D}^A))\bar{D}_1^R \\
\frac{d\bar{D}_{12}^R}{d\tau} &= (u_{10}^R + \alpha'(\bar{D}_2^R + \bar{D}_{12}^R))\bar{D}_2^R \\
&\quad + (u_{20}^R + \alpha(\bar{D}_2^R + \bar{D}_{12}^R) + \bar{\alpha}(\bar{D}_1^R + \bar{D}_{12}^R))\bar{D}_1^R \\
&\quad - (\mu'(\beta\varepsilon + \varepsilon'\bar{D}^A) + \mu(b\varepsilon + \varepsilon'\bar{D}^A))\bar{D}_{12}^R \\
\frac{d\bar{D}_2^R}{d\tau} &= (u_{20}^R + u_2^R + \alpha(\bar{D}_2^R + \bar{D}_{12}^R) + \bar{\alpha}(\bar{D}_1^R + \bar{D}_{12}^R))\bar{D} \\
&\quad + \mu'(\beta\varepsilon + \varepsilon'\bar{D}^A)\bar{D}_{12}^R - (u_{10}^R + \alpha'(\bar{D}_2^R + \bar{D}_{12}^R))\bar{D}_2^R \\
&\quad - \mu(b\varepsilon + \varepsilon'\bar{D}^A)\bar{D}_2^R \\
\frac{d\bar{D}^A}{d\tau} &= (u_0^A + u^A + \bar{D}^A)\bar{D} \\
&\quad - (\varepsilon + \varepsilon'(\bar{D}_2^R + \bar{D}_{12}^R) + \varepsilon'(\bar{D}_1^R + \bar{D}_{12}^R))\bar{D}^A,
\end{aligned} \tag{3}$$

with $\bar{D} = 1 - \bar{D}_1^R - \bar{D}_{12}^R - \bar{D}_2^R - \bar{D}^A$ (see [11] for the complete derivation and Table I for definition of reaction rate constants). It is important to point out that, in this model, if the gene expression is governed by a constitutive promoter, i.e., a promoter continuously active in standard conditions, without relying on external activators, then a constant non-basal *de-novo* establishment term for $\mathrm{D^A}$, u^A, must be considered.

A. Effect of epigenetic modifiers on model parameters

In order to determine how chromatin modifications alone (i.e., without permanent external inputs) affect gene expression memory, in our model we consider only epigenetic modifiers that are temporarily present in the system. From an experimental point of view, one method to temporarily introduce epigenetic modifiers into the system is transient transfection. With this method, the concentration of epigenetic modifiers will gradually decrease due to dilution until it completely vanishes.

Starting with H3K9me3 establishment, this aspect can be integrated into the model by writing the reaction rate constant of H3K9me3 establishment (k_W^2, see Table I) as $k_W^2 = \tilde{k}_W^2 W_2 e^{-\delta t}$. Here, W_2 is the total amount of the epigenetic modifier enhancing H3K9me3 establishment, such as KRAB [17], $\tilde{k}_W^2$ is a parameter independent of W_2, and δ denotes the dilution rate constant. The normalized input u_2^R in (3) can then be written as

$$u_2^R = \frac{k_W^2}{k_M^A D_{tot}} = \frac{\tilde{k}_W^2}{k_M^A}\frac{W_2}{D_{tot}}e^{-\delta t} = \tilde{u}_2^R \bar{W}_2 e^{-\varepsilon\tau}, \tag{4}$$

with $\tilde{u}_2^R = \tilde{k}_W^2/k_M^A$ and $\bar{W}_2 = W_2/D_{tot}$.

Similarly, the expression for the reaction rate constant of DNA methylation establishment (k_W^1, see Table I) can be written as $k_W^1 = \tilde{k}_W^1 W_1 e^{-\delta t}$. Here, W_1 is the total amount of DNMT3A, DNA methyltransferase that establishes *de novo* DNA methylation [1], and $\tilde{k}_W^1$ is a parameter independent of W_1. The normalized input u_1^R in the ODEs (3) can then be written as

$$u_1^R = \frac{k_W^1}{k_M^A D_{tot}} = \frac{\tilde{k}_W^1}{k_M^A}\frac{W_1}{D_{tot}}e^{-\delta t} = \tilde{u}_1^R \bar{W}_1 e^{-\varepsilon\tau}, \tag{5}$$

with $\tilde{u}_1^R = \tilde{k}_W^1/k_M^A$ and $\bar{W}_1 = W_1/D_{tot}$.

Finally, the expression for the reaction rate constants of DNA demethylation processes (k'_T and $k_T^{'*}$, see Table I) can be written as $k'_T = k'_{T1} + \tilde{k}'_T T e^{-\delta t}$ and $k_T^{'*} = k_{T1}^{'*} + \tilde{k}_T^{'*} T e^{-\delta t}$. Here, T is the total amount of the transiently transfected modifier that catalyzes DNA demethylation, such as TET1 [3], [15], k'_{T1} ($k_{T1}^{'*}$)

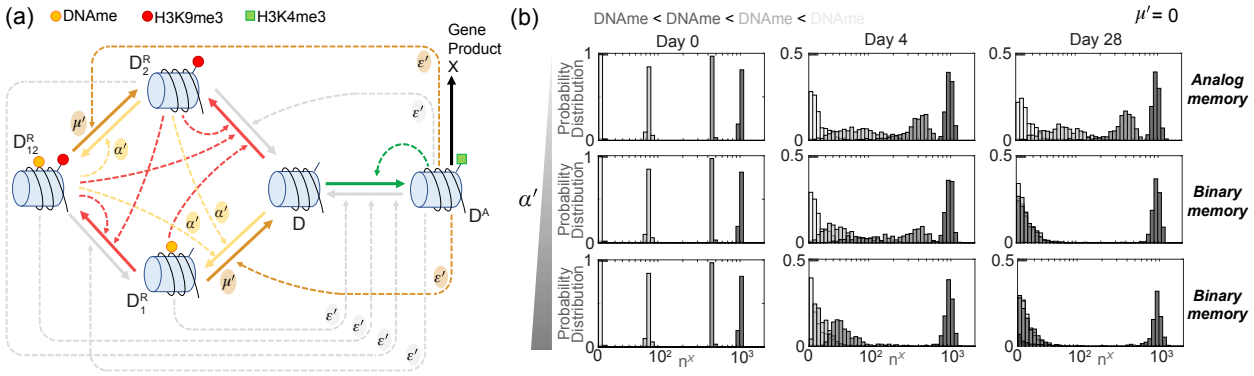

Fig. 1: Analog memory can be achieved when H3K9me3 does not catalyze DNA methylation (DNAme) establishment, i.e., when $\alpha' = 0$. (a) Diagram of complete chromatin modification circuit. The species are unmodified nucleosome (D), nucleosome with H3K4me3 (D^A), with DNAme (D_1^R), with H3K9me3 (D_2^R), and with both H3K9me3 and DNAme (D_{12}^R). Here, solid arrows denote the nucleosome modification processes and gene expression, while dashed arrows denote the enzyme recruitment processes. We use red for processes involved in H3K9me3 establishment, light (dark) orange for processes involved in DNAme establishment (DNA demethylation), green for processes involved in H3K4me3 establishment, gray for processes involved in the erasure of histone modifications, and black for gene expression. **(b)** Probability distributions of the system represented by reactions in Tables I, II for different values of α'. The distributions are obtained computationally using SSA [10] and we denote the gene expression level as n^X (logicle scale). The parameter values used are listed in Section VI-C. In particular, we consider $\alpha' = 0, 0.01, 0.1$ and four initial conditions: (n_{12}^R,n_1^R,n_2^R,n^A) = (14,0,1,0), (6,0,8,1), (4,0,5,6), and (1,0,1,13), going from light to dark gray, respectively. For all the simulations, we set $\mu' = 0$, $\alpha = \bar{\alpha} = 1$, $\varepsilon = 0.08$, $\varepsilon' = 25$, $\mu = 0.1$, $b = \beta = 1$, and $\mathrm{D_{tot}} = 15$ Finally, to realize each distribution, we conduct $N = 1000$ simulations.

is the component of the rate coefficient that does not depend on the external TET1 transfected, and $\tilde{k}'_T, \tilde{k}'^*_T$ are parameters independent of T. The parameter μ' in the ODEs (3) can then be written as

$$\begin{aligned}\mu' &= \frac{k'^*_T}{k^A_E} = \frac{k'^*_{T1}}{k^A_E} + \frac{\tilde{k}'^*_T D_{tot}}{k^A_E}\frac{T}{D_{tot}}e^{-\delta t} \\ &= \mu'_1 + \tilde{\mu}'\bar{T}e^{-\varepsilon\tau}, \end{aligned} \tag{6}$$

with $\mu'_1 = \frac{k'^*_{T1}}{k^A_E}$, $\tilde{\mu}'$, and $\bar{T} = T/D_{tot}$.

III. Gene Expression Model

During gene expression, DNA is first transcribed into mRNA m (transcription), that is then translated into the gene product X (translation). Chromatin modifications, by regulating DNA compaction, affect transcription and then gene expression [1], [18]. Therefore, we assume that transcription is predominantly allowed by D^A, while allowing a low level of transcription to all the other species. Additionally, m decay depends on dilution, due to cell division, and degradation, while X decay depends only on dilution [19] (see reactions in Table II). Introducing the non-dimensional parameters $\bar{\beta}^A_m = \beta^A_m/k^A_M D_{tot}$, $\bar{\beta}_m = \beta_m/k^A_M D_{tot}$, $\bar{\beta} = \beta/k^A_M D_{tot}$, $\bar{\gamma}_m = \gamma_m/k^A_M D_{tot}$, $\bar{\delta} = \delta/k^A_M D_{tot}$, the gene expression ODE model can be written as

$$\begin{aligned}\frac{d\bar{m}}{d\tau} &= \bar{\beta}^A_m \bar{D}^A + \bar{\beta}_m(\bar{D} + \bar{D}^R_1 + \bar{D}^R_2 + \bar{D}^R_{12}) - \bar{\gamma}_m \bar{m}, \\ \frac{d\bar{X}}{d\tau} &= \bar{\beta}\bar{m} - \bar{\delta}\bar{X}. \end{aligned} \tag{7}$$

IV. Impact of α' on the System's Behavior

We start our analysis by studying the stochastic behavior of the full model, i.e., model combining the complete chromatin modification circuit model with the gene expression model, with the aim of understanding the impact of α' (normalized rate of DNA methylation establishment catalyzed by H3K9me3) on the gene expression level probability distribution and, therefore, on the nature of gene expression memory achievable.

In particular, let us consider the parameter regime in which $\mu' = 0$, i.e., the DNA demethylation rate can be considered as approximately zero compared to histone modification erasure rate. This is because, without external epigenetic modifiers, it has been shown that the (passive) DNA demethylation process is significantly slow [8], [20]. When $\mu' = 0$, analog memory can be achieved only when $\alpha' = 0$, that is, when H3K9me3 does not recruit DNAme writers (Fig. 1(b)). In fact, in this parameter regime, after an initial diffusion phase, simulated cells maintain their set gene expression level. For $\alpha' > 0$, the gene expression level shifts either to a low or a high level. Furthermore, the higher α', the more the distribution tends to shift towards a low gene expression level (Fig. 1(b)).

Overall, these results suggest we can have analog memory only when DNA demethylation rate is sufficiently small compared to histone modification dynamics (that is, $\mu' \approx 0$) and H3K9me3 does not catalyze DNAme establishment ($\alpha' = 0$).

A. Analog memory captured by a reduced 2D chromatin modification circuit model

When these parameter conditions are verified and external epigenetic modifiers are not introduced into the system, the total number of nucleosomes with DNAme remains constant. More precisely, denoting the fraction of nucleosomes with DNAme in the gene of interest as $\bar{Y}_1 = \bar{D}_1^R + \bar{D}_{12}^R$, then we can define epigenetic cell memory as *analog* if $\bar{Y}_1(t) = \bar{Y}_1(0)$ for any $\bar{Y}_1 \in [0,1]$. In this case, the dynamics of the original model (3) can be described by a reduced 2D ODE model. Before deriving the reduced model, let us first merge into a unique rate the rates associated with the catalysis of H3K9me3 establishment by $\bar{D}_{12}^R$ and assume that this is equal to the rate of H3K9me3 establishment by $\bar{D}_1^R$. Similarly, let us merge the rates associated with the erasure of H3K4me3 by $\bar{D}_{12}^R$ and assume that this rate is equal to the erasure rate of H3K4me3 by $\bar{D}_1^R$. These simplifying assumptions do not affect the qualitative results related to the effect of the interactions among chromatin modifications on epigenetic cell memory. The ODE model (3) can then be rewritten as

$$\begin{aligned}
\frac{d\bar{D}_1^R}{d\tau} &= (u_{10}^R + u_1^R + \alpha'(\bar{D}_2^R + \bar{D}_{12}^R))\bar{D} + \mu(b\varepsilon + \varepsilon'\bar{D}^A)\bar{D}_{12}^R \\
&\quad - (u_{20}^R + \alpha(\bar{D}_2^R + \bar{D}_{12}^R) + \bar{\alpha}(\bar{D}_1^R + \bar{D}_{12}^R))\bar{D}_1^R \\
&\quad - \mu'(\beta\varepsilon + \varepsilon'\bar{D}^A))\bar{D}_1^R \\
\frac{d\bar{D}_{12}^R}{d\tau} &= (u_{10}^R + \alpha'(\bar{D}_2^R + \bar{D}_{12}^R))\bar{D}_2^R \\
&\quad + (u_{20}^R + \alpha\bar{D}_2^R + \bar{\alpha}(\bar{D}_1^R + \bar{D}_{12}^R))\bar{D}_1^R \\
&\quad - (\mu'(\beta\varepsilon + \varepsilon'\bar{D}^A) + \mu(b\varepsilon + \varepsilon'\bar{D}^A))\bar{D}_{12}^R \qquad (8) \\
\frac{d\bar{D}_2^R}{d\tau} &= (u_{20}^R + u_2^R + \alpha\bar{D}_2^R + \bar{\alpha}(\bar{D}_1^R + \bar{D}_{12}^R))\bar{D} \\
&\quad + \mu'(\beta\varepsilon + \varepsilon'\bar{D}^A)\bar{D}_{12}^R - (u_{10}^R + \alpha'(\bar{D}_2^R + \bar{D}_{12}^R))\bar{D}_2^R \\
&\quad - \mu(b\varepsilon + \varepsilon'\bar{D}^A)\bar{D}_2^R \\
\frac{d\bar{D}^A}{d\tau} &= (u_0^A + u^A + \bar{D}^A)\bar{D} \\
&\quad - (\varepsilon + \varepsilon'(\bar{D}_2^R) + \varepsilon'(\bar{D}_1^R + \bar{D}_{12}^R))\bar{D}^A,
\end{aligned}$$

Now, let us introduce the following proposition:

Proposition IV.1. *Let $\alpha' = c\mu_1'$, with $c = O(1)$, and let us consider the following system, shown in Fig. 2(a):*

$$\begin{aligned}
\frac{d\bar{D}_2^R}{d\tau} &= (\alpha\bar{D}_2^R + \bar{\alpha}\bar{Y}_1)\bar{D} - \mu(b\varepsilon + \varepsilon'\bar{D}^A)\bar{D}_2^R, \qquad (9) \\
\frac{d\bar{D}^A}{d\tau} &= (u^A + \bar{D}^A)\bar{D} - (\varepsilon + \varepsilon'(\bar{D}_2^R + \bar{Y}_1))\bar{D}^A,
\end{aligned}$$

with $\bar{D} = 1 - \bar{D}^A - \bar{D}_2^R - \bar{Y}_1$ and $\bar{Y}_1 = constant$. Then, for sufficiently small μ_1' and $\alpha' = c\mu_1'$, any $(\bar{D}_2^R(\tau,\mu_1'), \bar{D}^A(\tau,\mu_1'))$ from the solution of (8) *can be expressed with the following expansions:*

$$\bar{D}_2^R(\tau,\mu_1') = \bar{D}_2^{R^*}(\tau) + O(\mu_1'),$$

$$\bar{D}^A(\tau,\mu_1') = \bar{D}^{A*}(\tau) + O(\mu_1'), \qquad (10)$$

in which $(\bar{D}_2^{R^*}(\tau), \bar{D}^{A*}(\tau))$ is the solution of (9) *and with the error estimate holding as $\mu_1' \to 0$ uniformly for $0 \le \tau \le T$.*

Proof. Let us first rewrite system (8) by assuming negligible basal *de novo* establishment ($u_{10}^R = u_{20}^R = u_0^A = 0$) and introducing the variable $\bar{Y}_1 = \bar{D}_1^R + \bar{D}_{12}^R$:

$$\begin{aligned}
\frac{d\bar{Y}_1}{d\tau} &= (u_1^R)\bar{D} + (\alpha'(\bar{D}_2^R + \bar{D}_{12}^R))(\bar{D} + \bar{D}_2^R) \\
&\quad - \mu'(\beta\varepsilon + \varepsilon'\bar{D}^A)\bar{Y}_1 \\
\frac{d\bar{D}_{12}^R}{d\tau} &= (\alpha'(\bar{D}_2^R + \bar{D}_{12}^R))\bar{D}_2^R + (\alpha\bar{D}_2^R + \bar{\alpha}\bar{Y}_1)\bar{D}_1^R \\
&\quad - (\mu'(\beta\varepsilon + \varepsilon'\bar{D}^A) + \mu(b\varepsilon + \varepsilon'\bar{D}^A))\bar{D}_{12}^R \qquad (11) \\
\frac{d\bar{D}_2^R}{d\tau} &= (u_2^R + \alpha\bar{D}_2^R + \bar{\alpha}\bar{Y}_1)\bar{D} + \mu'(\beta\varepsilon + \varepsilon'\bar{D}^A)\bar{D}_{12}^R \\
&\quad - (\alpha'(\bar{D}_2^R + \bar{D}_{12}^R) + \mu(b\varepsilon + \varepsilon'\bar{D}^A))\bar{D}_2^R \\
\frac{d\bar{D}^A}{d\tau} &= (u^A + \bar{D}^A)\bar{D} - (\varepsilon + \varepsilon'\bar{D}_2^R + \varepsilon'\bar{Y}_1)\bar{D}^A,
\end{aligned}$$

in which $\bar{D} = 1 - \bar{Y}_1 - \bar{D}_2^R - \bar{D}^A$ and $\bar{D}_1^R = \bar{Y}_1 - \bar{D}_{12}^R$. Now, let us introduce in (11) the expressions for u_2^R, u_1^R, and μ' derived in Section II-A (Eqs (4) - (6)):

$$\begin{aligned}
\frac{d\bar{Y}_1}{d\tau} &= \tilde{u}_1^R\bar{W}_1 e^{-\varepsilon\tau}\bar{D} + (\alpha'(\bar{D}_2^R + \bar{D}_{12}^R))(\bar{D} + \bar{D}_2^R) \\
&\quad - (\mu_1' + \tilde{\mu}'\bar{T}e^{-\varepsilon\tau})(\beta\varepsilon + \varepsilon'\bar{D}^A)\bar{Y}_1 \\
\frac{d\bar{D}_{12}^R}{d\tau} &= (\alpha'(\bar{D}_2^R + \bar{D}_{12}^R))\bar{D}_2^R + (\alpha\bar{D}_2^R + \bar{\alpha}\bar{Y}_1)\bar{D}_1^R \\
&\quad - (\mu_1' + \tilde{\mu}'\bar{T}e^{-\varepsilon\tau})(\beta\varepsilon + \varepsilon'\bar{D}^A)\bar{D}_{12}^R \\
&\quad - \mu(b\varepsilon + \varepsilon'\bar{D}^A)\bar{D}_{12}^R \qquad (12) \\
\frac{d\bar{D}_2^R}{d\tau} &= (\tilde{u}_2^R\bar{W}_2 e^{-\varepsilon\tau} + \alpha\bar{D}_2^R + \bar{\alpha}\bar{Y}_1)\bar{D} \\
&\quad + (\mu_1' + \tilde{\mu}'\bar{T}e^{-\varepsilon\tau})(\beta\varepsilon + \varepsilon'\bar{D}^A)\bar{D}_{12}^R \\
&\quad - (\alpha'(\bar{D}_2^R + \bar{D}_{12}^R) + \mu(b\varepsilon + \varepsilon'\bar{D}^A))\bar{D}_2^R \\
\frac{d\bar{D}^A}{d\tau} &= (u^A + \bar{D}^A)\bar{D} - (\varepsilon + \varepsilon'\bar{D}_2^R + \varepsilon'\bar{Y}_1)\bar{D}^A.
\end{aligned}$$

After a temporary phase, during which the external inputs gradually decrease until they completely vanish ($e^{-\varepsilon\tau} \approx 0$), system (12) can be rewritten as

$$\begin{aligned}
\frac{d\bar{Y}_1}{d\tau} &= \alpha'(\bar{D}_2^R + \bar{D}_{12}^R)(\bar{D} + \bar{D}_2^R) - \mu_1'(\beta\varepsilon + \varepsilon'\bar{D}^A)\bar{Y}_1 \\
\frac{d\bar{D}_{12}^R}{d\tau} &= (\alpha'(\bar{D}_2^R + \bar{D}_{12}^R))\bar{D}_2^R + (\alpha\bar{D}_2^R + \bar{\alpha}\bar{Y}_1)\bar{D}_1^R \\
&\quad - (\mu_1'(\beta\varepsilon + \varepsilon'\bar{D}^A) + \mu(b\varepsilon + \varepsilon'\bar{D}^A))\bar{D}_{12}^R \qquad (13) \\
\frac{d\bar{D}_2^R}{d\tau} &= (\alpha\bar{D}_2^R + \bar{\alpha}\bar{Y}_1)\bar{D} + \mu_1'(\beta\varepsilon + \varepsilon'\bar{D}^A)\bar{D}_{12}^R \\
&\quad - (\alpha'(\bar{D}_2^R + \bar{D}_{12}^R) + \mu(b\varepsilon + \varepsilon'\bar{D}^A))\bar{D}_2^R \\
\frac{d\bar{D}^A}{d\tau} &= (u^A + \bar{D}^A)\bar{D} - (\varepsilon + \varepsilon'\bar{D}_2^R + \varepsilon'\bar{Y}_1)\bar{D}^A.
\end{aligned}$$

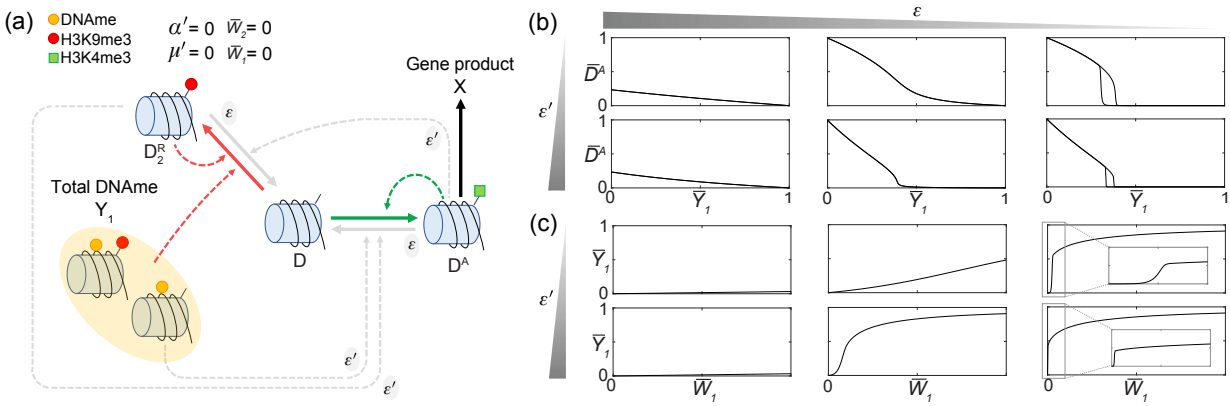

Fig. 2: Effect of basal erasure basal erasure and (ε) and mutual inhibition between activating and repressive marks (ε') on the response between H3K4me3 ($\bar{D}^A$), DNA methylation grade ($\bar{Y}_1$) at the gene, and initial level of DNA methylation writer DNMT3A ($\bar{W}_1$). (a) Simplified chromatin modification circuit diagram obtained when $\alpha' = 0$, $\mu' = 0$, $\bar{W}_1 = 0$, and $\bar{W}_2 = 0$. **(b)** Dose-response curve for $(\bar{Y}_1, \bar{D}^A)$ for different values of ε and ε', obtained from simulations of system (9) with $(\bar{Y}_1, \bar{D}_2^R, \bar{D}^A) = (j, 0, 1-j)$ as initial conditions, with $0 \leq j \leq 1$. **(c)** Dose-response curve for $(\bar{W}_1, \bar{Y}_1)$, for different values of ε and ε' obtained from simulations of system (9), with $d\bar{Y}_1/d\tau = \tilde{u}_1^R \bar{W}_1 e^{-\varepsilon\tau}\bar{D}$ and setting $(\bar{Y}_1, \bar{D}_2^R, \bar{D}^A) = (0, 0, 1)$ as initial condition and $\bar{W}_1 = [0, 4]$. For panels (b) and (c), we consider $\varepsilon = 0.0001, 0.1, 50$ and $\varepsilon' = 1, 25$. The other parameter values are $\beta = 1$, $\tilde{u}_1^R = 1$, $\alpha = \bar{\alpha} = 1$, $\mu = 0.1$, $b = 1$, $u^A = 15$. Here, the external input dynamics is modeled as a pulse that exponentially decreases over time and $\bar{W}_1$ corresponds to the external input value at time 0. In our model, α' is the normalized rate of DNAme establishment catalyzed by H3K9me3, μ' quantifies the relative speed between the rate of DNA demethylation and the activating modification erasure rate, and ε (ε') is the parameter scaling the rate of the basal erasure process (recruited erasure process) with respect to the auto-catalysis rate of each chromatin mark.

Now, let us set $\mu_1' = 0$ (and then $\alpha' = c\mu_1' = 0$):

$$\begin{aligned}
\frac{d\bar{Y}_1}{d\tau} &= 0 \\
\frac{d\bar{D}_{12}^R}{d\tau} &= (\alpha\bar{D}_2^R + \bar{\alpha}\bar{Y}_1)\bar{D}_1^R - \mu(b\varepsilon + \varepsilon'\bar{D}^A)\bar{D}_{12}^R \quad (14)\\
\frac{d\bar{D}_2^R}{d\tau} &= (\alpha\bar{D}_2^R + \bar{\alpha}\bar{Y}_1)\bar{D} - (\mu(b\varepsilon + \varepsilon'\bar{D}^A))\bar{D}_2^R \\
\frac{d\bar{D}^A}{d\tau} &= (u^A + \bar{D}^A)\bar{D} - (\varepsilon + \varepsilon'\bar{D}_2^R + \varepsilon'\bar{Y}_1)\bar{D}^A,
\end{aligned}$$

in which $\bar{D} = 1 - \bar{Y}_1 - \bar{D}_2^R - \bar{D}^A$ and $\bar{D}_1^R = \bar{Y}_1 - \bar{D}_{12}^R$. From (14), it follows that $\bar{Y}_1 = constant$. This implies that, during the transient phase in which external inputs are introduced into the system, $\bar{Y}_1$ evolves according to $d\bar{Y}_1/d\tau = \tilde{u}_1^R \bar{W}_1 e^{-\varepsilon\tau}\bar{D}$ until $e^{-\varepsilon\tau} \approx 0$, at which point $\bar{Y}_1$ reaches a certain value. Now, let us define $x = (\bar{Y}_1, \bar{D}_{12}^R, \bar{D}_2^R, \bar{D}^A)$, and denote as $f(x, \mu_1')$ ($f(x, 0)$) the matrix in which each row corresponds to the right-hand side of each equation in (13) (in (14)). Then, it is evident that $f(x, \mu_1')$ and $f(x, 0)$ are smooth functions of their variables. Furthermore, since each entry of $\partial f(x, 0)/\partial x$ is bounded for any x, we have that $||\partial f(x, 0)/\partial x||_2 < L$, with $L > 0$ being a real number. From this, it follows that there exists a unique solution $x_0(\tau)$ for the system (14) on the interval $0 \leq \tau \leq T$ (Existence-Uniqueness Theorem, [21]). We can then conclude that system (13) is regularly perturbed, with small parameter μ_1', and its solution can be expressed as a Taylor expansion $x(\tau, \mu_1') = x_0(\tau) + O(\mu_1')$ [22]. In particular, since the last two ODEs in (14) depend only on $\bar{D}_2^R$, $\bar{D}^A$, and $\bar{Y}_1$, once the external inputs die out ($e^{-\varepsilon\tau} \approx 0$), $\bar{Y}_1$ remains constant and the dynamics of ($\bar{D}^A$, $\bar{D}_2^R$) can be expressed as a series expansion as the one described in (10), in which $(\bar{D}_2^{R^*}(\tau), \bar{D}^{A*}(\tau))$ is the solution of the reduced 2D ODE model represented by the last two equations in (14), coinciding with the ODEs in (9). □

Overall, this model reduction shows that, in the parameter regime in which analog memory can be achieved (i.e., $\mu' = 0$, $\alpha' = 0$), the DNA methylation grade remains constant, and the chromatin modification circuit dynamics is dictated by the evolution of histone modifications. Therefore, we can use this simpler, reduced model to determine the conditions under which analog memory leads to bimodal probability distributions of gene expression level, and then validate these findings through a computational study of the full model.

V. Impact of ε and ε' on the system's behavior

Let us now consider the analog memory parameter regime (i.e., $\mu' = 0$, $\alpha' = 0$) and study the deterministic and stochastic behavior of our system, with the aim of understanding the impact of ε and ε' on the probability distribution of gene expression levels. As a reminder, ε and ε' are parameters scaling the rate of the basal erasure process and recruited erasure process, respectively, with respect to the auto-catalysis rate of each chromatin mark.

We start by studying the reduced 2D ODE model (Eqs (9)) in order to determine the effect of ε and ε'

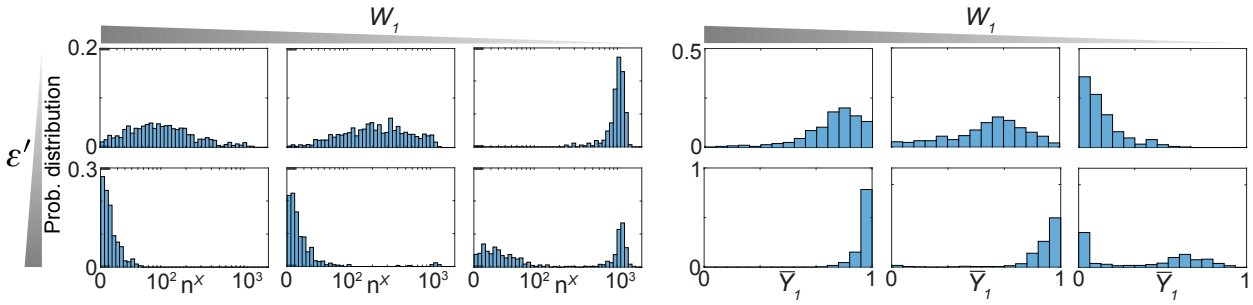

Fig. 3: The ultrasensitive response between the level of DNA methylation writer DNMT3A and DNA methylation grade leads to a bimodal distribution of gene expression levels. Probability distributions of the system represented by reactions in Tables I and II, after 28 days. We obtained them using SSA [10]. More precisely, on the left-hand side we have gene expression level probability distribution (logicle scale) and on the right-hand side we have the total DNAme level probability distributions. The parameter values used to generate these plots are listed in Section VI-C. In particular, we consider $\varepsilon = 0.13$, $\varepsilon' = 1.5, 25$ and $(n_{12}^R, n_1^R, n_2^R, n^A) = (0, 0, 0, \mathrm{D_{tot}})$ as initial condition. We consider $\mathrm{D_{tot}} = 15$, $N = 1000$ simulations to generate each distribution and, for each simulation conducted, the value of $\bar{W}_1$ was randomly selected from a uniformly distributed range, whose extremes are $\bar{W}_1 = [0, 0.4], [2.4, 2.8], [3.4, 3.8]$, respectively.

on the value of $\bar{D}^A$ at the equilibrium for different $\bar{Y}_1$, i.e., fractions of DNAme in the gene (Fig. 2(b)). For large values of ε, the system has a unique stable steady state characterized by low $\bar{D}^A$, with $\bar{D}^A$ decreasing as $\bar{Y}_1$ increases (Fig. 2(b)). As ε decreases, the value of D^A at steady-state increases, especially when $\bar{Y}_1$ is low, where $\bar{D}^A \approx 1$ (Fig. 2(b)). Reducing ε even further leads the system to be bistable for intermediate values of $\bar{Y}_1$ (Fig. 2(b)). Varying ε' does not significantly affect these trends, except when ε is small. In such cases, larger ε' leads to a smaller range of $\bar{Y}_1$ in which the system is bistable and to a smaller difference in the values of $\bar{D}^A$ between the two steady states (Fig. 2(b)). The second analysis aims to understand how ε and ε' affect the level of DNAme $\bar{Y}_1$ at equilibrium for various initial levels of $\bar{W}_1$, denoting DNAme writer DNMT3A (Fig. 2(c)). The analysis shows that larger values of $\bar{W}_1$ enable reaching higher values of $\bar{Y}_1$. Furthermore, when ε is low, high values of $\bar{Y}_1$ can be achieved, and, in case of small ε, higher ε' results in a more ultrasensitive curve (Fig. 2(c)).

Overall, these results suggest that high fractions of nucleosomes with H3K4me3, and consequently high levels of gene expression, are possible only for sufficiently small values of ε (Fig. 2(b)). In this parameter regime, when ε' is sufficiently high, $\bar{Y}_1$ shows an ultrasensitive response to transient dosage of DNAme writer DNMT3A. As a result, different ranges of values of initial DNMT3A transfection levels (W_1) would result only in either low or high gene expression levels (Fig. 2(b),(c)). To validate these results, we conduct a computational study on the full model, whose reactions are listed in Tables I, II (Fig. 3), using SSA [10]. For different ranges of initial DNMT3A levels (W_1), we obtain a bimodal probability distribution of gene expression levels when ε' is sufficiently large. For smaller values of ε', the stationary distribution shifts towards a unimodal shape, in agreement with our expectations derived from our deterministic analysis (Fig. 2(b),(c)).

This analysis suggests that an ultrasensitive response between DNMT3A and DNA methylation grade, along with intrinsic noise, leads to a bimodal gene expression level distribution when the external input DNMT3A is randomly selected from a range of values uniformly distributed. Due to this ultrasensitivity, most simulations conducted exhibit either high or low DNA methylation levels, corresponding to low or high gene expression levels, while some simulations show intermediate DNA methylation levels, leading to intermediate gene expression levels (Fig. 2(b),(c)). Therefore, in the obtained gene expression level bimodal distribution, simulated cells are not predominantly in the high and low states, with cells in the intermediate states corresponding to those oscillating between the two states, consistent with the binary memory hypothesis. Instead, each simulated cell, including those associated with intermediate gene expression levels, maintains its initial gene expression level based on the DNA methylation grade achieved after the initial transient phase.

VI. Concluding Remarks and Discussion

In this work, we introduce and analyze a mathematical model combining histone modifications and DNA methylation, derived starting from the one in [11] (Sections II, III) to determine how chromatin modifications affect the memory of gene expression levels. Our results show that, without external inputs (epigenetic modifiers), analog memory of gene expression can be achieved when DNA methylation level in the gene of interest remains constant at any initially set level. This phenomenon is observed when H3K9me3 does not catalyze *de novo* DNA methylation, i.e., $\alpha' = 0$, and DNA

methylation decay rate is negligible, i.e., $\mu' = 0$ (Section IV, Fig. 1(b)). Our results also show that in the parameter regime compatible with analog memory, transiently applied external inputs lead to a bimodal distribution, recapitulating those observed experimentally [8], only when ε is sufficiently small and ε' is sufficiently large. In this case, cells do not oscillate between high and low gene expression states, but maintain their initial gene expression level based on the DNA methylation grade achieved after the initial transient phase.

Overall, our results suggest the mechanisms determining when epigenetic cell memory is analog, highlighting the key role of DNA methylation.

It is important to note that when α' is extremely small, but non-zero, analog memory may still be achieved, but only for a finite duration. More precisely, the closer α' is to zero, the longer the temporal duration of analog gene expression states (Fig. 1(b)). This is because, when H3K9me3 mediates the establishment of DNA methylation, DNA methylation itself is subject to positive feedback. When this positive feedback is sufficiently strong (α' sufficiently high), then binary memory emerges after a certain interval of time, and fully methylated or completely unmethylated states become the only heritable states (Fig. 1(b)).

Given that the interactions between DNA methylation and histone modifications are context-dependent [23], it is plausible that different patterns of such interactions arise in distinct cellular and genetic contexts. Then, we expect that the specific cellular and genetic context will determine the strength by which H3K9me3 mediates DNA methylation establishment (parameter α'), and hence influencing the temporal duration of analog gene expression states. This context-dependence may also explain why the expression of fate-specific genes is binary in some cell types while appearing continuous in others [9].

Previous experimental studies confirm the weak catalysis of DNA methylation by H3K9me3 ($\alpha' = 0$) in certain cell types [8]. Furthermore, a previous computational study suggests that long-term memory of silenced and active gene expression levels can be achieved only for sufficiently small values of ε [11], [24]. Additional experiments are underway and preliminary results largely confirm the theoretical findings [25]. Our model and our theoretical results could help discern the nature of gene expression memory (analog or binary) and the contributions of DNA methylation and histone modifications to it.

APPENDIX

A. Chromatin modification circuit: reaction list

The reaction model describing the complete chromatin modification circuit can be written as in Table I.

$\mathbf{R}_j$	**Reaction**	**Prop.Func.**(a_j)	**Param.**
1	$\mathrm{D} \xrightarrow{k^A_{W0}} \mathrm{D^A}$	$a_1 = k^A_{W0} n^D$	k^A_{W0}
2	$\mathrm{D} \xrightarrow{k^A_W} \mathrm{D^A}$	$a_2 = k^A_W n^D$	k^A_W
3	$\mathrm{D^A} \xrightarrow{\bar{k}^A_E} \mathrm{D}$	$a_3 = \bar{k}^A_E n^A$	$\bar{k}^A_E$
4	$\mathrm{D^A} \xrightarrow{\delta} \mathrm{D}$	$a_4 = \delta n^A$	δ
5	$\mathrm{D} + \mathrm{D^A} \xrightarrow{k^A_M} \mathrm{D^A} + \mathrm{D^A}$	$a_5 = \frac{k^A_M}{\Omega} n^D n^A$	$\frac{k^A_M}{\Omega}$
6	$\mathrm{D^A} + \mathrm{D^R_1} \xrightarrow{k^A_E} \mathrm{D} + \mathrm{D^R_1}$	$a_6 = \frac{k^A_E}{\Omega} n^A n^R_1$	$\frac{k^A_E}{\Omega}$
7	$\mathrm{D^A} + \mathrm{D^R_{12}} \xrightarrow{k^A_E} \mathrm{D} + \mathrm{D^R_{12}}$	$a_7 = \frac{k^A_E}{\Omega} n^A n^R_{12}$	$\frac{k^A_E}{\Omega}$
8	$\mathrm{D^A} + \mathrm{D^R_2} \xrightarrow{k^A_E} \mathrm{D} + \mathrm{D^R_2}$	$a_8 = \frac{k^A_E}{\Omega} n^A n^R_2$	$\frac{k^A_E}{\Omega}$
9	$\mathrm{D^A} + \mathrm{D^R_{12}} \xrightarrow{k^A_E} \mathrm{D} + \mathrm{D^R_{12}}$	$a_9 = \frac{k^A_E}{\Omega} n^A n^R_{12}$	$\frac{k^A_E}{\Omega}$
10	$\mathrm{D} \xrightarrow{k^1_{W0}} \mathrm{D^R_1}$	$a_{10} = k^1_{W0} n^D$	k^1_{W0}
11	$\mathrm{D} \xrightarrow{k^1_W} \mathrm{D^R_1}$	$a_{11} = k^1_W n^D$	k^1_W
12	$\mathrm{D^R_1} \xrightarrow{k'_T} \mathrm{D}$	$a_{12} = k'_T n^R_1$	k'_T
13	$\mathrm{D^R_1} \xrightarrow{\delta'} \mathrm{D}$	$a_{13} = \delta' n^R_1$	δ'
14	$\mathrm{D} + \mathrm{D^R_2} \xrightarrow{k'_M} \mathrm{D^R_1} + \mathrm{D^R_2}$	$a_{14} = \frac{k'_M}{\Omega} n^D n^R_2$	$\frac{k'_M}{\Omega}$
15	$\mathrm{D} + \mathrm{D^R_{12}} \xrightarrow{k'_M} \mathrm{D^R_1} + \mathrm{D^R_{12}}$	$a_{15} = \frac{k'_M}{\Omega} n^D n^R_{12}$	$\frac{k'_M}{\Omega}$
16	$\mathrm{D^R_1} + \mathrm{D^A} \xrightarrow{k'^*_T} \mathrm{D} + \mathrm{D^A}$	$a_{16} = \frac{k'^*_T}{\Omega} n^R_1 n^A$	$\frac{k'^*_T}{\Omega}$
17	$\mathrm{D} \xrightarrow{k^2_{W0}} \mathrm{D^R_2}$	$a_{17} = k^2_{W0} n^D$	k^2_{W0}
18	$\mathrm{D} \xrightarrow{k^2_W} \mathrm{D^R_2}$	$a_{18} = k^2_W n^D$	k^2_W
19	$\mathrm{D^R_2} \xrightarrow{\bar{k}^R_E} \mathrm{D}$	$a_{19} = \bar{k}^R_E n^R_2$	$\bar{k}^R_E$
20	$\mathrm{D^R_2} \xrightarrow{\delta} \mathrm{D}$	$a_{20} = \delta n^R_2$	δ
21	$\mathrm{D} + \mathrm{D^R_2} \xrightarrow{k_M} \mathrm{D^R_2} + \mathrm{D^R_2}$	$a_{21} = \frac{k_M}{\Omega} n^D n^R_2$	$\frac{k_M}{\Omega}$
22	$\mathrm{D} + \mathrm{D^R_{12}} \xrightarrow{k_M} \mathrm{D^R_2} + \mathrm{D^R_{12}}$	$a_{22} = \frac{k_M}{\Omega} n^D n^R_{12}$	$\frac{k_M}{\Omega}$
23	$\mathrm{D} + \mathrm{D^R_1} \xrightarrow{\bar{k}_M} \mathrm{D^R_2} + \mathrm{D^R_1}$	$a_{23} = \frac{\bar{k}_M}{\Omega} n^D n^R_1$	$\frac{\bar{k}_M}{\Omega}$
24	$\mathrm{D} + \mathrm{D^R_{12}} \xrightarrow{\bar{k}_M} \mathrm{D^R_2} + \mathrm{D^R_{12}}$	$a_{24} = \frac{\bar{k}_M}{\Omega} n^D n^R_{12}$	$\frac{\bar{k}_M}{\Omega}$
25	$\mathrm{D^R_2} + \mathrm{D^A} \xrightarrow{k^R_E} \mathrm{D} + \mathrm{D^A}$	$a_{25} = \frac{k^R_E}{\Omega} n^R_2 n^A$	$\frac{k^R_E}{\Omega}$
26	$\mathrm{D^R_1} \xrightarrow{k^2_{W0}} \mathrm{D^R_{12}}$	$a_{26} = k^2_{W0} n^R_1$	k^2_{W0}
27	$\mathrm{D^R_{12}} \xrightarrow{\bar{k}^R_E} \mathrm{D^R_1}$	$a_{27} = \bar{k}^R_E n^R_{12}$	$\bar{k}^R_E$
28	$\mathrm{D^R_{12}} \xrightarrow{\delta} \mathrm{D^R_1}$	$a_{28} = \delta n^R_{12}$	δ
29	$\mathrm{D^R_1} + \mathrm{D^R_2} \xrightarrow{k_M} \mathrm{D^R_{12}} + \mathrm{D^R_2}$	$a_{29} = \frac{k_M}{\Omega} n^R_1 n^R_2$	$\frac{k_M}{\Omega}$
30	$\mathrm{D^R_1} + \mathrm{D^R_{12}} \xrightarrow{k_M} \mathrm{D^R_{12}} + \mathrm{D^R_{12}}$	$a_{30} = \frac{k_M}{\Omega} n^R_1 n^R_{12}$	$\frac{k_M}{\Omega}$
31	$\mathrm{D^R_1} + \mathrm{D^R_1} \xrightarrow{\bar{k}_M} \mathrm{D^R_{12}} + \mathrm{D^R_1}$	$a_{31} = \frac{\bar{k}_M}{\Omega} \frac{n^R_1(n^R_1-1)}{2}$	$\frac{\bar{k}_M}{\Omega}$
32	$\mathrm{D^R_1} + \mathrm{D^R_{12}} \xrightarrow{\bar{k}_M} \mathrm{D^R_{12}} + \mathrm{D^R_{12}}$	$a_{32} = \frac{\bar{k}_M}{\Omega} n^R_1 n^R_{12}$	$\frac{\bar{k}_M}{\Omega}$
33	$\mathrm{D^R_{12}} + \mathrm{D^A} \xrightarrow{k^R_E} \mathrm{D^R_1} + \mathrm{D^A}$	$a_{33} = \frac{k^R_E}{\Omega} n^R_{12} n^A$	$\frac{k^R_E}{\Omega}$
34	$\mathrm{D^R_2} \xrightarrow{k^1_{W0}} \mathrm{D^R_{12}}$	$a_{34} = k^1_{W0} n^R_2$	k^1_{W0}
35	$\mathrm{D^R_{12}} \xrightarrow{k'_T} \mathrm{D^R_2}$	$a_{35} = k'_T n^R_{12}$	k'_T
36	$\mathrm{D^R_{12}} \xrightarrow{\delta'} \mathrm{D^R_2}$	$a_{36} = \delta' n^R_{12}$	δ'
37	$\mathrm{D^R_2} + \mathrm{D^R_2} \xrightarrow{k'_M} \mathrm{D^R_{12}} + \mathrm{D^R_2}$	$a_{37} = \frac{k'_M}{\Omega} \frac{n^R_2(n^R_2-1)}{2}$	$\frac{k'_M}{\Omega}$
38	$\mathrm{D^R_2} + \mathrm{D^R_{12}} \xrightarrow{k'_M} \mathrm{D^R_{12}} + \mathrm{D^R_{12}}$	$a_{38} = \frac{k'_M}{\Omega} n^R_2 n^R_{12}$	$\frac{k'_M}{\Omega}$
39	$\mathrm{D^R_{12}} + \mathrm{D^A} \xrightarrow{k'^*_T} \mathrm{D^R_2} + \mathrm{D^A}$	$a_{39} = \frac{k'^*_T}{\Omega} n^R_{12} n^A$	$\frac{k'^*_T}{\Omega}$

TABLE I: Full chromatin modification circuit model: reactions

B. Gene expression: reaction list

The reaction model associated with gene expression can be written as in Table II. In particular, defining the transcription rate constants as β^A_m and β_m, we assume

$\mathbf{R}_j$	**Reaction**	**Prop.Func.**(a_j)	**Param.**
1	$\mathrm{D^A} \xrightarrow{\beta_m^A} \mathrm{D^A + m}$	$a_1 = \beta_m^A n^A$	β_m^A
2	$\mathrm{D} \xrightarrow{\beta_m} \mathrm{D + m}$	$a_2 = \beta_m n^D$	β_m
3	$\mathrm{D_1^R} \xrightarrow{\beta_m} \mathrm{D_1^R + m}$	$a_3 = \beta_m n_1^R$	β_m
4	$\mathrm{D_2^R} \xrightarrow{\beta_m} \mathrm{D_2^R + m}$	$a_4 = \beta_m n_2^R$	β_m
5	$\mathrm{D_{12}^R} \xrightarrow{\beta_m} \mathrm{D_{12}^R + m}$	$a_5 = \beta_m n_{12}^R$	β_m
6	$\mathrm{m} \xrightarrow{\beta} \mathrm{m + X}$	$a_6 = \beta n^m$	β
7	$\mathrm{m} \xrightarrow{\gamma_m} \emptyset$	$a_7 = \gamma_m n^m$	γ_m
8	$\mathrm{X} \xrightarrow{\delta} \emptyset$	$a_8 = \delta n^X$	δ

TABLE II: Gene expression model: reactions

$\beta_m < \beta_m^A$ (see Section III).

C. Parameter values used in the simulations

Simulations in Fig. 1: $k_{W0}^A = 0$, $k_W^A = 7.8075$ h^{-1}, $\bar{k}_E^A = 0.0118$ h^{-1}, $\delta = 0.0291$ h^{-1}, $\frac{k_M^A}{\Omega} = 0.0347$ h^{-1}, $\frac{k_E^A}{\Omega} = 0.8675$ h^{-1}, $k_{W0}^1 = k_W^1 = 0$, $k_T' = 0$, $\delta' = 0$, $\frac{k_M'}{\Omega} = 0, 3.47 \cdot 10^{-4}, 3.47 \cdot 10^{-3}$ h^{-1}, $\frac{k_T'^*}{\Omega} = 0$, $k_{W0}^2 = k_W^2 = 0$, $\bar{k}_E^R = 0.0012$ h^{-1}, $\frac{k_M}{\Omega} = 0.0347$ h^{-1}, $\frac{\bar{k}_M}{\Omega} = 0.0347$ h^{-1}, $\frac{k_E^R}{\Omega} = 0.0868$ h^{-1}, $\beta_m = 0.2556$ h^{-1}, $\beta_m^A = 0.0021$ h^{-1}, $\beta = 2.52$ h^{-1}, $\gamma_m = 0.24$ h^{-1}.
Simulations in Fig. 3: $k_{W0}^A = 0$, $k_W^A = 7.8075$ h^{-1}, $\bar{k}_E^A = 0.0315$ h^{-1}, $\delta = 0.035$ h^{-1}, $\frac{k_M^A}{\Omega} = 0.0347$ h^{-1}, $\frac{k_E^A}{\Omega} = 0.0520, 0.8675$ h^{-1}, $k_{W0}^1 = 0$, $k_W^1 \in [0, 0.3643]e^{-\delta t}, [0.2602, 0.6246]e^{-\delta t}, [0.5205, 0.885]e^{-\delta t}$ h^{-1}, $k_T' = 0$, $\delta' = 0$, $\frac{k_M'}{\Omega} = 0$, $\frac{k_T'^*}{\Omega} = 0$, $k_{W0}^2 = k_W^2 = 0$, $\bar{k}_E^R = 0.0032$ h^{-1}, $\frac{k_M}{\Omega} = 0.0347$ h^{-1}, $\frac{\bar{k}_M}{\Omega} = 0.0347$ h^{-1}, $\frac{k_E^R}{\Omega} = 0.0052, 0.0868$ h^{-1}, $\beta_m = 0.2556$ h^{-1}, $\beta_m^A = 0.0021$ h^{-1}, $\beta = 2.52$ h^{-1}, $\gamma_m = 0.24$ h^{-1}. In the simulations of both figures, we set, as initial value for n^X of n^m, their steady states of the ODEs.

REFERENCES

[1] C. D. Allis, M.-L. Caparros, T. Jenuwein, and D. Reinberg, *Epigenetics*. Cold Spring Harbor Laboratory Press, Second Edition, 2015.

[2] N. Carey, *The epigenetic revolution*. Columbia University Press, 2013.

[3] S. Huang, M. Litt, and C. A. Blakey, *Epigenetic Gene Expression and Regulation*. Academic Press, 2015.

[4] E. Li and Y. Zhang, "Dna methylation in mammals," *Cold Spring Harb Perspect Biol*, vol. 6, no. 5, 2014.

[5] A. P. Bird and M. H. Taggart, "Variable patterns of total dna and rdna methylation in animals," *Nucleic Acids Res*, vol. 8, no. 7, pp. 1485–1497, 1980.

[6] E. Hodges, A. Molaro, C. O. Dos Santos, P. Thekkat, Q. Song, P. J. Uren, J. Park, J. Butler, S. Rafii, W. R. McCombie, A. D. Smith, and G. J. Hannon, "Dna methylation changes and complex intermediate states accompany lineage specificity in the adult hematopoietic compartment," *Molecular cell*, vol. 44, no. 1, pp. 17–28, 2011.

[7] M. B. Stadler, R. Murr, L. Burger, R. Ivanek, F. Lienert, A. Schöler, E. van Nimwegen, C. Wirbelauer, E. J. Oakeley, D. Gaidatzis, T. V. Tiwari, and D. Schübeler, "Dna-binding factors shape the mouse methylome at distal regulatory regions," *Nature*, vol. 480, no. 7378, pp. 490–495, 2011.

[8] L. Bintu, J. Yong, Y. E. Antebi, K. McCue, Y. Kazuki, N. Uno, M. Oshimura, and M. B. Elowitz, "Dynamics of epigenetic regulation at the single-cell level," *Science*, 2016.

[9] Z. Yao, C. T. J. van Velthoven, T. N. Nguyen, J. Goldy, A. E. Sedeno-Cortes, F. Baftizadeh, D. Bertagnolli, T. Casper, M. Chiang, K. Crichton, S.-L. Ding, O. Fong, E. Garren, A. Glandon, N. W. Gouwens, J. Gray, L. T. Graybuck, M. J. Hawrylycz, D. Hirschstein, M. Kroll, K. Lathia, C. Lee, B. Levi, D. McMillen, S. Mok, T. Pham, Q. Ren, C. Rimorin, N. Shapovalova, J. Sulc, S. M. Sunkin, M. Tieu, A. Torkelson, H. Tung, K. Ward, N. Dee, K. A. Smith, B. Tasic, and H. Zeng, "A taxonomy of transcriptomic cell types across the isocortex and hippocampal formation," *Cell*, vol. 184, no. 12, pp. 3222–3241, 2021.

[10] D. T. Gillespie, "Stochastic simulation of chemical kinetics," *Annual Review of Physical Chemistry*, vol. 58, no. 1, pp. 35–55, 2007.

[11] S. Bruno, R. J. Williams, and D. Del Vecchio, "Epigenetic cell memory: The gene's inner chromatin modification circuit," *PLOS Computational Biology*, vol. 18, no. 4, pp. 1 – 27, 2022.

[12] T. Zhang, S. Cooper, and N. Brockdorff, "The interplay of histone modifications - writers that read," *EMBO Rep*, vol. 16, no. 11, pp. 1467–1481, 2015.

[13] F. Fuks, P. J. Hurd, D. Wolf, X. Nan, A. P. Bird, and T. Kouzarides, "The methyl-cpg-binding protein mecp2 links dna methylation to histone methylation," *J Biol Chem*, vol. 278, no. 6, pp. 4035–4040, 2003.

[14] A. K. Upadhyay, J. R. Horton, X. Zhang, and X. Cheng, "Coordinated methyl-lysine erasure: structural and functional linkage of a jumonji demethylase domain and a reader domain," *Curr Opin Struct Biol*, vol. 21, no. 6, pp. 750–60, 2011.

[15] K. D. Rasmussen and K. Helin, "Role of tet enzymes in dna methylation, development, and cancer," *Genes Dev.*, vol. 30, no. 7, pp. 733–50, 2016.

[16] D. A. Brown, V. D. Cerbo, A. Feldmann, J. Ahn, S. Ito, N. P. Blackledge, M. Nakayama, M. McClellan, E. Dimitrova, A. H. Turberfield, H. K. Long, H. W. King, S. Kriaucionis, L. Schermelleh, T. G. Kutateladze, H. Koseki, and R. J. Klose, "The set1 complex selects actively transcribed target genes via multivalent interaction with cpg island chromatin," *Cell Rep*, vol. 20, no. 10, pp. 2313–2327, 2017.

[17] D. C. Schultz, K. Ayyanathan, D. Negorev, G. G. Maul, and F. J. Rauscher, "Setdb1: a novel kap-1-associated histone h3, lysine 9-specific methyltransferase that contributes to hp1-mediated silencing of euchromatic genes by krab zinc-finger proteins," *Annual Review of Physical Chemistry*, vol. 16, no. 8, pp. 919–32, 2002.

[18] K. L. Huisinga, B. Brower-Toland, and S. C. Elgin, "The contradictory definitions of heterochromatin: transcription and silencing," *Chromosoma*, vol. 115, no. 2, pp. 110–22, 2006.

[19] D. Del Vecchio and R. M. Murray, *Biomolecular Feedback Systems*. Princeton University Press, 2014.

[20] M. Jackson, A. Krassowska, N. Gilbert, T. Chevassut, L. Forrester, J. Ansell, and B. Ramsahoye, "Severe global dna hypomethylation blocks differentiation and induces histone hyperacetylation in embryonic stem cells," *Mol Cell Biol*, vol. 24, no. 20, 2004.

[21] E. A. Coddington and N. Levinson, *Theory of Ordinary Differential Equations*. McGraw-Hill, 1955.

[22] F. C. Hoppensteadt, *Regular Perturbation Methods*, pp. 139–156. New York, NY: Springer New York, 1993.

[23] A. L. Mattei, N. Bailly, and A. Meissner, "Dna methylation: a historical perspective," *Trends Genet*, vol. 38, no. 7, pp. 676–707, 2022.

[24] S. Bruno, R. J. Williams, and D. Del Vecchio, "Model reduction and stochastic analysis of the histone modification circuit," in *2022 European Control Conference (ECC)*, pp. 264–271, 2022.

[25] S. Palacios, S. Bruno, R. Weiss, E. Salibi, A. Kane, K. Ilia, and D. D. Vecchio, "Analog epigenetic cell memory by graded dna methylation," *bioRxiv*, 2024.